Supporting Information

Intrinsic Color Sensing System Allows for Real-Time Observable Functional Changes on Human Induced Pluripotent Stem Cell Derived Cardiomyocytes

Yiqi Gong[1,‡], Zhuoyue Chen[2,3‡], Li Yang[4], Xuefeng Ai[1], Bingqian Yan[1,5], Huijing Wang[5], Liya Qiu[6], Yao Tan[1,5], Nevin Witman[7], Wei Wang[1,], Yuanjin Zhao[2,*], Wei Fu[1,5,8*]*

[1]Department of Pediatric Cardiothoracic Surgery, Shanghai Children's Medical Center, School of Medicine, Shanghai Jiao Tong University, 1678 Dong Fang Road, Shanghai 200127, China.

[2]Department of Clinical Laboratory, The Affiliated Drum Tower Hospital of Nanjing University Medical School, Nanjing 210008, China.

[3]State Key Laboratory of Bioelectronics, School of Biological Science and Medical Engineering, Southeast University, Nanjing 210096, China

[4]Department of Anesthesiology, Fudan University Shanghai Cancer Center; Department of Oncology, Shanghai Medical College, Fudan University, No. 270, Dong An Road, Shanghai 200032, China.

[5]Institute of Pediatric Translational Medicine, Shanghai Children's Medical Center, School of Medicine, Shanghai Jiao Tong University, 1678 Dong Fang Road, Shanghai

200127, China.

[6]Shanghai Institute of Technical Physics of the Chinese Academy of Sciences, Shanghai 200083, China.

[7]Department of Medicine, Karolinska Institutet; Department of Cell and Molecular Biology, Karolinska Institutet, Stockholm, 171 77, Sweden.

[8]Shanghai Key Laboratory of Tissue Engineering, Shanghai 9th People's Hospital, School of Medicine, Shanghai Jiao Tong University, Shanghai 200011, China

‡These authors contributed equally to this work.

*Corresponding authors: wangwei@scmc.com.cn (Wei Wang); yjzhao@seu.edu.cn (Yuanjin Zhao); fuweizhulu@163.com (Wei Fu)

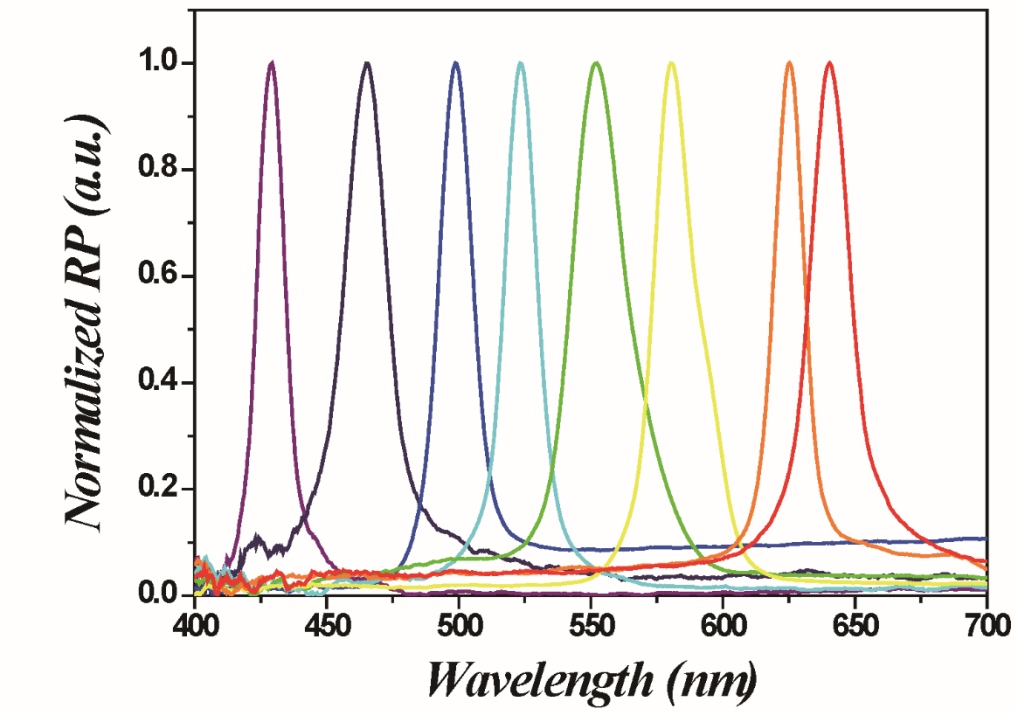

Figure S1. Spectra of Different Colloidal Crystal Templates with Different Sizes of Silica Nanoparticles.

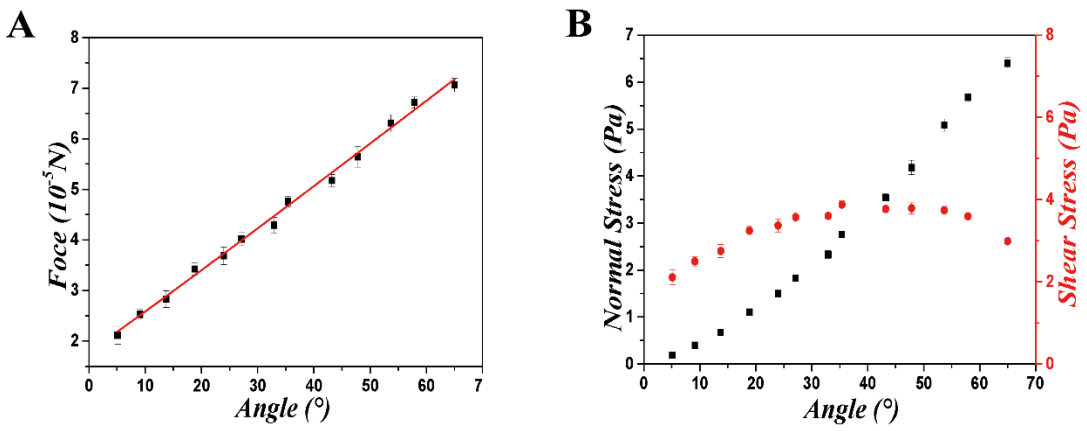

Figure S2. The Relationship Between Force and Bending Angle of the Structural Color GelMA. (A) The relationship between the external applied force and the bending angle of the GelMA hydrogel strip (20 mm in length, 50mm in width and 0.85mm in thickness). (B) The relationship between normal stress (in black), shear stress (in red) and bending angle of the GelMA hydrogel.

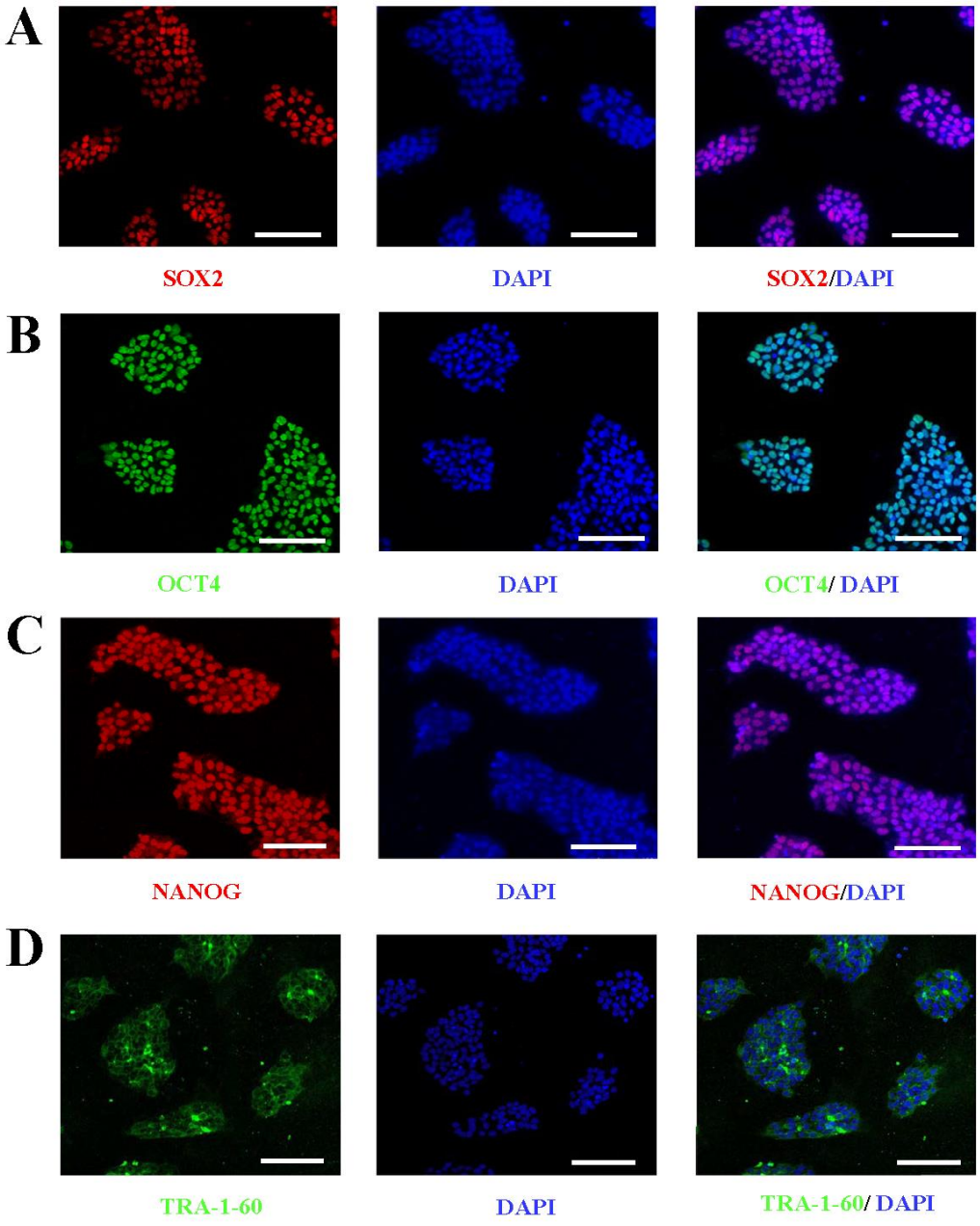

Figure S3. The Molecular Validation of Human Induced Pluripotent Stem Cells. (A) Immunofluorescence staining of SOX2. (B) Immunofluorescence staining of OCT4. (C) Immunofluorescence staining of NANOG. (D) Immunofluorescence staining of TRA-1-60. Scale bar, 100μm.

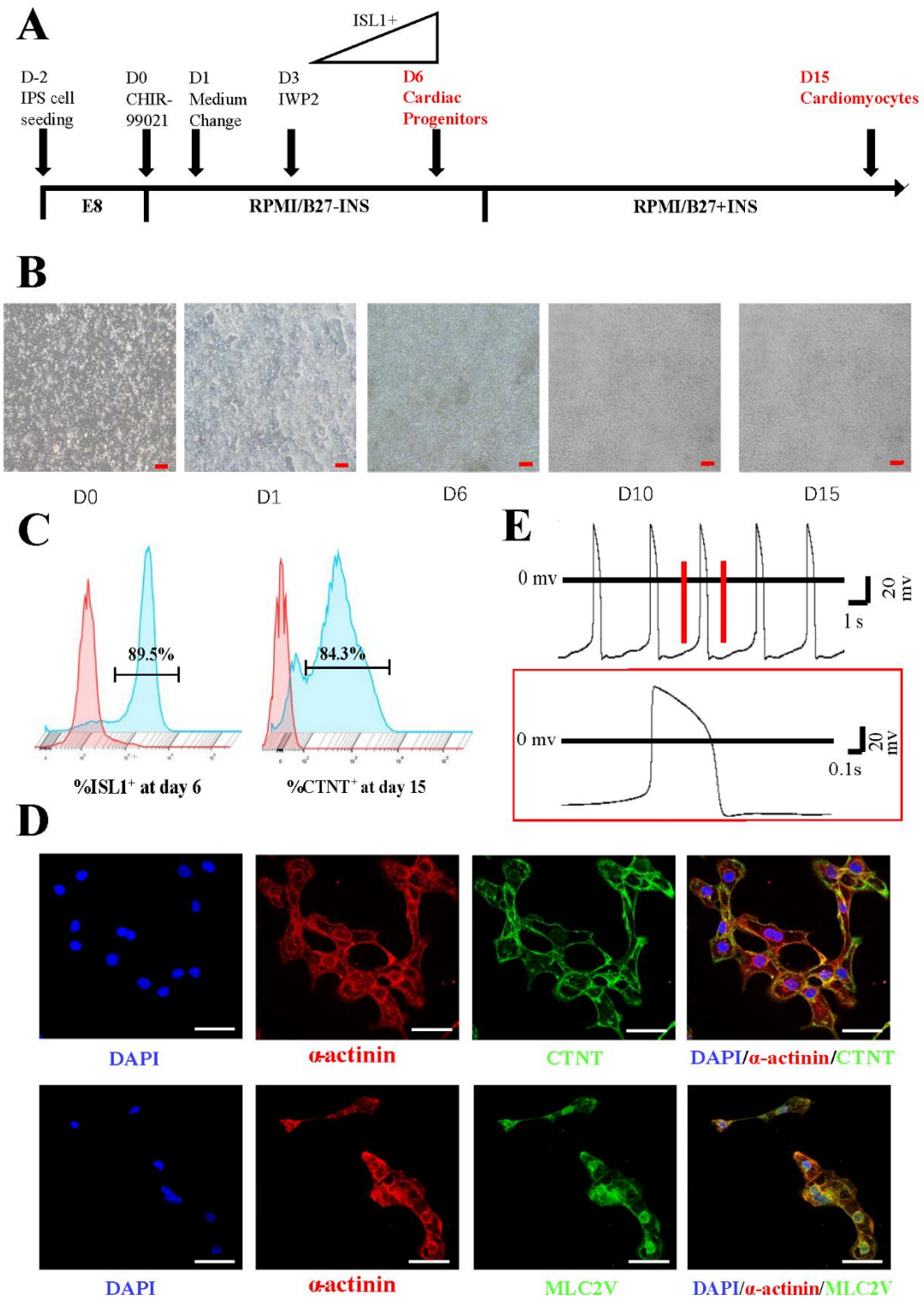

Figure S4. Generation and Identification of hiPSC-Derived Cardiac Progenitors and Cardiomyocytes. (A) Schematic of the differentiation protocol. (B) Phase contrast

images of cells during differentiation process. Scale bar, 200μm. (C) Percentage of $ISL1^+$ cardiac progenitors and $CTNT^+$ cardiomyocytes measured by flow cytometry on day 6 and day 15 of differentiation generated with the indicated methods, n=3 independent biological replicates. (D) Immunofluorescence staining for CTNT, α-actinin (cardiomyocyte structural markers), and MLC2V (ventricular cardiomyocytes). Scale bar, 10μm. (E) Typical action potential of an individual hiPSC–derived cardiomyocyte recorded *via* patch clamp (n = 15 cells). Inset, enlarged waveform of a single action potential. Solid line indicates resting potential at 0 mV.

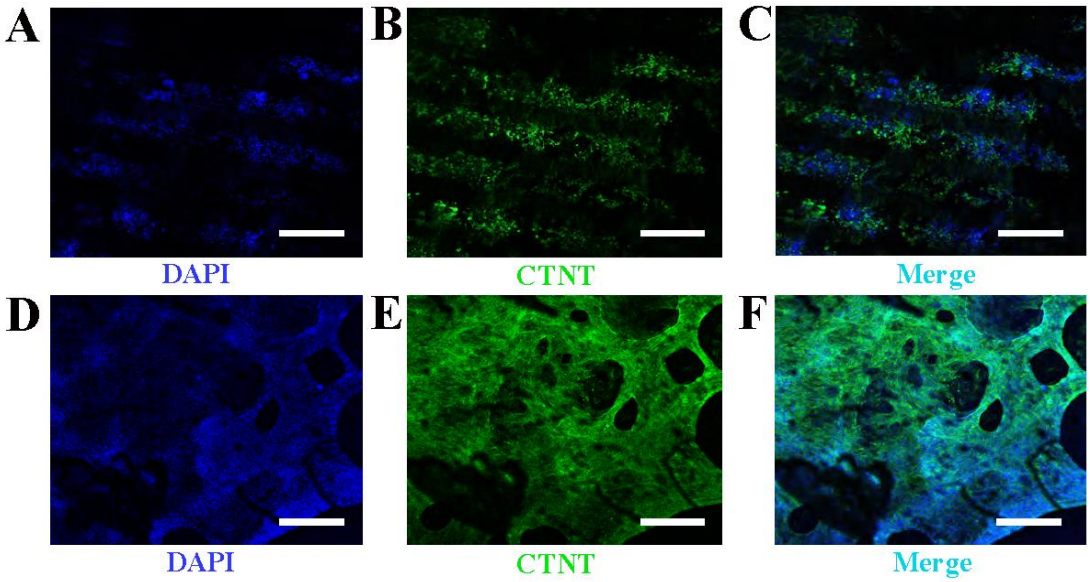

Figure S5. Cardiac Progenitors Cultured on Flat and Microgroove Structural Color GelMA Films and the Effect of the Topography on Cells. (A-C) hiPSC-CMs on microgroove structural color GelMA films on day 15. Aligned cell structure could be observed. Scale bar, 150μm. (D-F) hiPSC-CMs on flat structural color GelMA films on day 15. Random cell structure could be observed. Scale bar, 300μm.

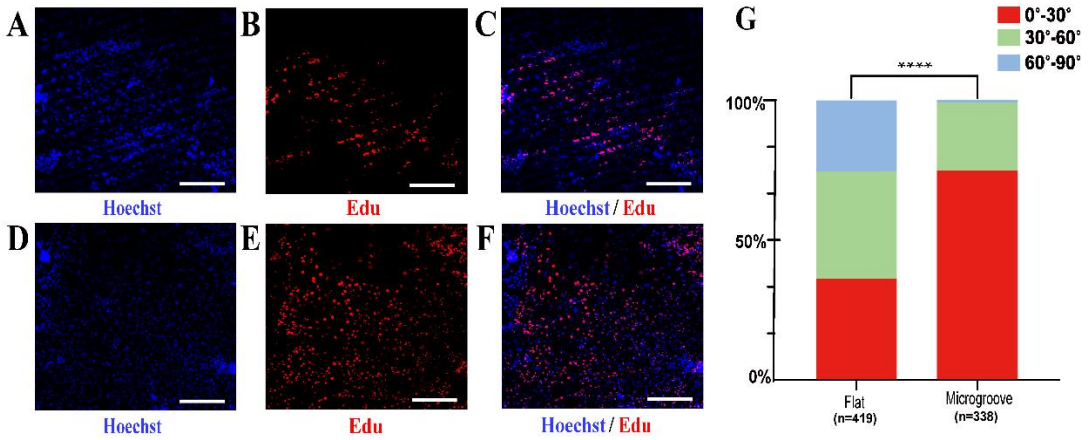

Figure S6. The Proliferation of Cells Cultured on Flat and Microgroove Structural Color GelMA Films. (A-C) Representative images of cell proliferation on the microgroove structural color GelMA films between day 13 and 15. Scale bar, 200μm. (D-F) Representative images of cell proliferation on the flat structural color GelMA films between day 13 and 15. Scale bar, 200μm. (G) Orientation angle frequency distribution of the hiPSC-CMs on flat and microgroove structural color GelMA films on day 15. **** $p < 0.001$

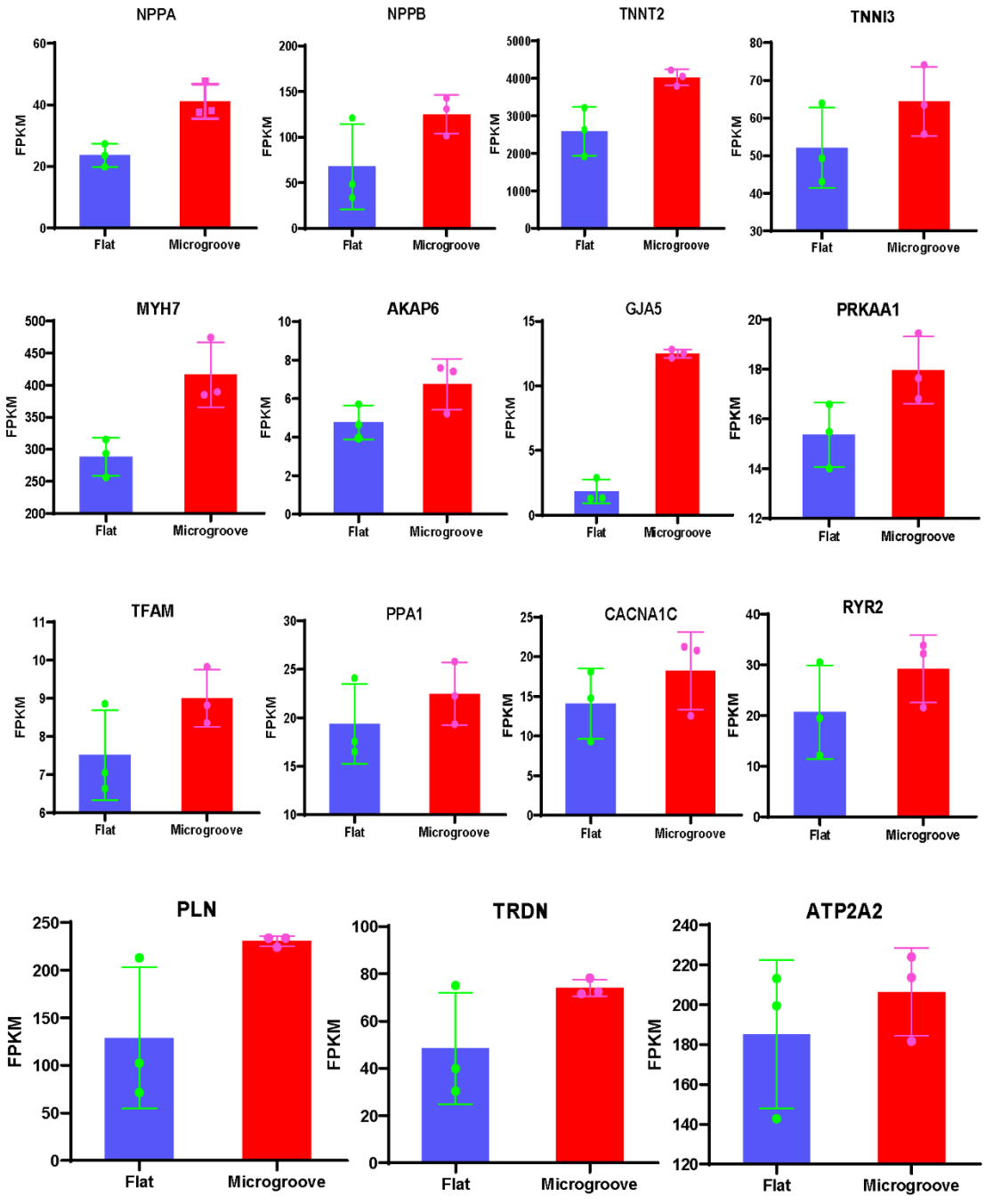

Figure S7. Functional Genes of Cells on the Microgroove Structural Color GelMA Films Up Regulated on Day 15 Comparing with on the Flat Structural Color GelMA Films.

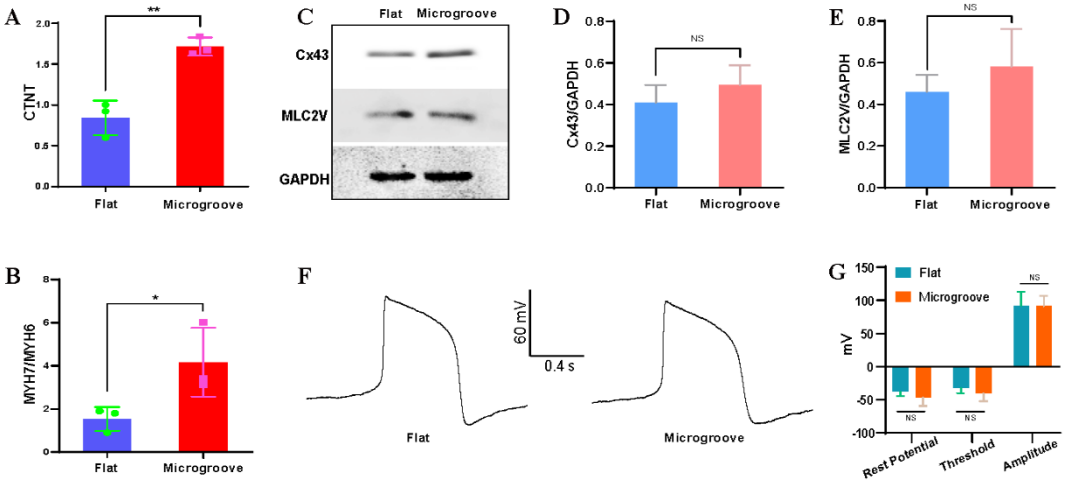

Figure S8. Representative Genes, Proteins and Electrophysiological Function Related to Cardiac Differentiation Expressed on Day 15 by hiPSC-CMs Cultured on Flat or Microgroove Structural Color GelMA. (A) Real time PCR analysis of the effect of microgroove structural color GelMA on the cardiomyocyte functional gene CTNT. n=3, ** $p < 0.01$. (B) Real time PCR analysis of the effect of microgroove on the cardiomyocyte functional gene MYH7/MYH6. * $p < 0.05$. (C-E) Western blot analysis of the effect of microgroove structural color GelMA on MLC2V and Cx43 protein expression. (F) The action potential waveforms of hiPSC-CMs cultured on flat or microgroove structural color GelMA on day 15. (G) The rest potential, threshold and amplitude of hiPSC-CMs cultured on flat or microgroove structural color GelMA on day 15.

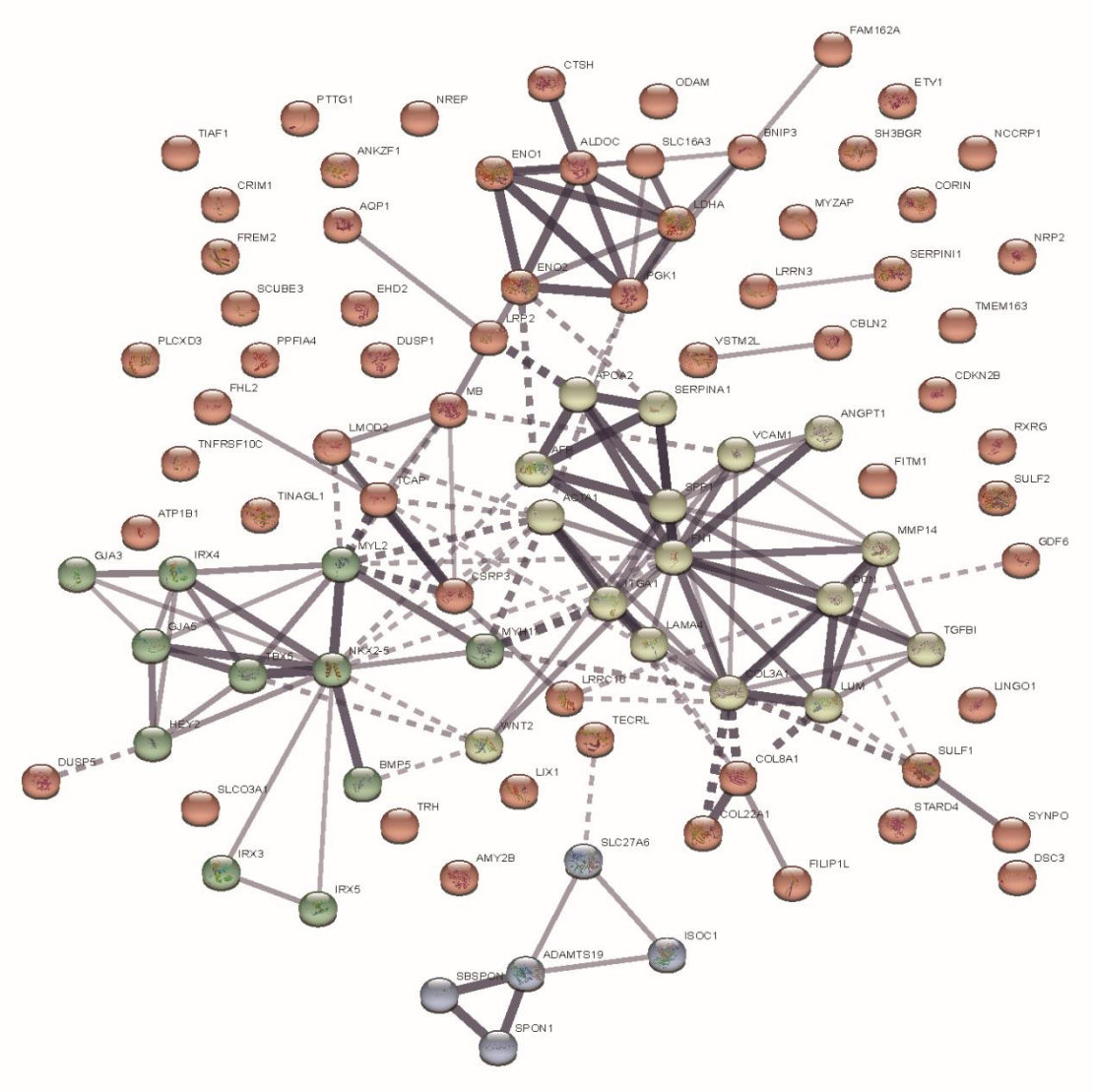

Figure S9. The Protein-Protein Interaction Network of the Differentially Expressed Genes on Day 15.

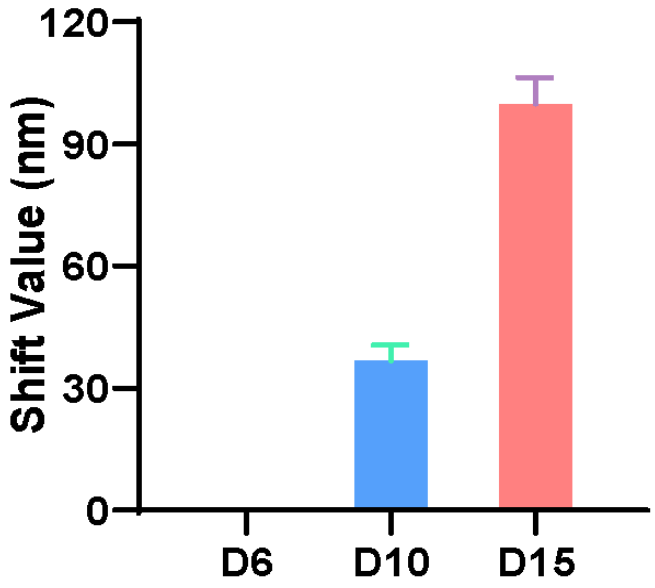

Figure S10. The Shift Values of Reflection Peaks During hCPCs Differentiation Process on Day 6, Day 10, Day 15. (n=4 independent repeated experiments)